J Nanostruct 15(4): 1774-1783, Autumn 2025

RESEARCH PAPER

Preparation and Characterization of PEG-Fe_3O_4 Nanocomposites as an Efficient Controlled Release System for Catechin

Balzhan Azimkhanova [1]*, Uday Abdul-Reda Hussein [2], Hayder Hamid Abbas Al-Anbari [3], Abed J. Kadhim [4], Mohammed Khudair [5], Talib Kh. Hussein [26], Sadiq H. Al-shaikh [7], Imad Ibrahim Dawood [8], Kamola Daminova [9], Nigina Mukhamadiyeva [10], Kamila Kaymanova [11], Kamol Xakimov [12], Sabokhat Sadikova [13]

[1] *Department of Biochemistry, Kazakh National Medical University, Almaty, Kazakhstan*

[2] *Department of Pharmaceutics, College of Pharmacy, University of Al-Ameed, Iraq*

[3] *Ahl Al bayt University, College of pharmacy/ Kerbala/ Iraq*

[4] *Department of Medical Laboratories Technology, Al-Nisour University College, Nisour Seq. Karkh, Baghdad, Iraq*

[5] *Warka University College, Iraq*

[6] *Al-Hadi University College, Baghdad, Iraq*

[7] *Department of Medical Laboratory Technics, Al-Zahrawi University College, Karbala, Iraq*

[8] *Mazaya University College, Iraq*

[9] *Department of Family Medicine, Clinical Pharmacology, Tashkent State Medical University, Republic of Uzbekistan*

[10] *Department of Psychiatry, Narcology and Medical Psychology, Bukhara State Medical Institute named after Abu Ali ibn Sino, Bukhara, Republic of Uzbekistan*

[11] *Department of Histology, Cytology and Embryology , Bukhara State Medical Institute named after Abu Ali ibn Sino, Bukhara, Republic of Uzbekistan*

[12] *Termez State University of Engineering and Agrotechnology, Termez, 190100, Uzbekistan*

[13] *Department of Chemistry, Urgench State University, Urgench, Uzbekistan*

ARTICLE INFO

Article History:
Received 14 June 2025
Accepted 07 September 2025
Published 01 October 2025

Keywords:
Catechin
Controlled release
Drug release
Magnetic nanocomposites
PEG-Fe_3O_4

ABSTRACT

This study reports the preparation, characterization, and evaluation of PEG-coated Fe_3O_4 magnetic nanocomposites as a stimuli-responsive platform for the controlled release of catechin. Magnetic Fe_3O_4 nanoparticles were synthesized by a coprecipitation method under inert conditions, followed by surface functionalization with poly(ethylene glycol) (PEG) to enhance colloidal stability, biocompatibility, and dispersibility in physiological media. The PEG-Fe_3O_4 nanocomposites were characterized by FE-SEM and FT-IR to confirm morphology, core–shell architecture, and successful PEG grafting. Catechin was loaded onto the PEG-Fe_3O_4 matrix via physical adsorption and hydrogen bonding, achieving loading efficiency of ~82% and a capacity of ~12.7 mg catechin per 100 mg nanocomposites. In vitro release studies under simulated physiological conditions (pH 7.4 PBS, 37 °C) demonstrated sustained catechin release with pH-responsive behavior: 58.3% release at 24 h at pH 7.4 versus 89.2% at pH 5.0, indicating enhanced release in acidic/tumor-like environments. Magnetic-field triggering further accelerated release (78.5% at 24 h under AMF). Release kinetics were best described by the Korsmeyer–Peppas model (R2 > 0.94), with diffusion and polymer relaxation contributing to release (n ~ 0.43–0.51). Stability assessments showed minimal iron leaching (<5%) over 48 h, and retained magnetic responsiveness for potential reuse. The results underscore PEG–Fe_3O_4 nanocomposites as versatile, stimuli-responsive carriers for catechin with potential applications in targeted and controlled nutraceutical or therapeutic delivery.

How to cite this article
Azimkhanova B., Hussein U., Al-Anbari H. et al. Preparation and Characterization of PEG-Fe_3O_4 Nanocomposites as an Efficient Controlled Release System for Catechin. J Nanostruct, 2025; 15(4):1774-1783. DOI: 10.22052/JNS.2025.04.025

* *Corresponding Author Email: sultanbaderaljehani@hotmail.com*

INTRODUCTION

Magnetic nanoparticles (MNPs), particularly Fe_3O_4-based systems, have emerged as versatile platforms in modern nano-medicine and materials science due to their unique superparamagnetic behavior, biocompatibility, and facile surface functionalization [1-5]. Their intrinsic magnetization enables external magnetic field–guided localization, rapid and reversible heating under alternating magnetic fields, and efficient separation from complex matrices, which collectively underpin a broad spectrum of applications in drug delivery and controlled release [6-8]. In drug delivery, MNPs facilitate targeted transport to diseased sites, minimize off-target exposure, and enable stimuli-responsive release when combined with surface coatings or responsive linkers [9-12]. Surface engineering with polymers [13], silica [14], or ligand moieties can endow biocompatibility, reduce opsonization, and provide functional handles for covalent drug conjugation or encapsulation, while preserving magnetic responsiveness for magnetic targeting and imaging. Beyond therapeutic delivery, Fe_3O_4-based nanocomposites are exploited in biosensing [15], catalysis [16], and environmental remediation [17], where their high surface area, easy recoverability, and tunable magnetic properties enable efficient separation and recyclability. Crucially, the integration of magnetic cores with polymeric, inorganic, or hybrid matrices affords composite systems that combine controlled swelling, diffusion-controlled release, and responsive behavior to pH, temperature, or redox conditions, thereby enabling precise control over drug release kinetics. The ongoing challenge remains to optimize colloidal stability, minimize cytotoxicity, and balance magnetic strength with payload capacity, but advances in surface chemistry and synthesis control continue to expand the utility of MNP-based platforms in both intracellular and extracellular contexts.

Controlled release (CR) drug delivery has evolved from early matrix systems and barrier-based designs to sophisticated, stimuli-responsive platforms that can modulate therapeutic exposure in time and space [18-21]. Historically, CR concepts emerged to mitigate peak-and-trough plasma levels, improve patient compliance, and reduce dosing frequency, with initial approaches focusing on diffusion-controlled polymers and reservoir devices. Over the decades, advances in polymer science [22, 23], nanotechnology [24], and materials engineering [25, 26] have enabled nuanced control over release kinetics through mechanisms such as diffusion, erosion, swelling, and biodegradation, often choreographed by environmental cues (pH, temperature, redox conditions) or external stimuli (magnetic, ultrasonic, light). In the context of poly(ethylene glycol) (PEG)–based and inorganic–organic hybrid systems, CR performance is increasingly governed by the interfacial design, particle size, surface chemistry, and matrix architecture, which collectively tune the diffusion path length, polymer relaxation, and payload stability. Catechin, a bioactive polyphenol with well-documented antioxidant, anti-inflammatory, and cardioprotective properties, presents challenges for conventional delivery due to limited aqueous solubility, stability under physiological conditions, and rapid metabolism (Figure 1). Recent developments in catechin CR focus on encapsulation within biocompatible carriers (liposomes, polymeric nanoparticles, mesoporous materials, and nanocomposites) to enhance solubility, protect against degradation, and achieve sustained, controlled release in response to physiological triggers [27-35]. Specifically, catechin release studies have highlighted strategies such as

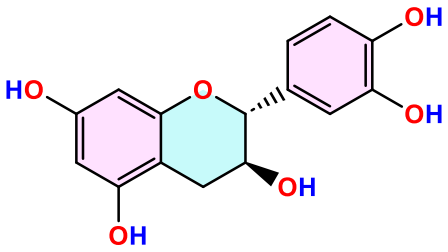

Fig. 1. The chemical structure of catechin.

crosslinked polymer matrices, surface-anchored functional groups, and stimuli-responsive linkers that delay release in circulation while enabling accelerated release at target sites. The integration of catechin with PEGylated, magnetic, or hybrid nanocomposites shows promise for achieving dual benefits: prolonged systemic residence due to stealth-like PEG coronae and on-demand release modulated by local magnetic or environmental cues. Ongoing challenges include achieving precise release kinetics across diverse physiological environments, ensuring biocompatibility and stability during storage, and translating laboratory-scale CR systems into scalable, clinically relevant formulations.

The aim of this study is to develop and characterize PEG-coated Fe_3O_4 magnetic nanocomposites as an efficient, stimuli-responsive controlled release system for catechin, enabling enhanced solubility, stability, and tunable release kinetics under biologically relevant conditions.

MATERIALS AND METHODS

General remarks

All chemicals were used as received unless otherwise stated. Catechin (≥98% purity, Cat. No. (7295-85-4) was purchased from Sigma-Aldrich, and polyethylene glycol with terminal amine or hydroxyl functionality (PEG, average molecular weight [6000 Mw], purity ≥ 98) was obtained from Sigma-Aldrich. Iron(II) sulfate heptahydrate ($FeSO_4 \cdot 7H_2O$, ≥99%), iron(III) chloride hexahydrate ($FeCl_3 \cdot 6H_2O$, ≥99%), ammonium hydroxide solution (NH_4OH, 28–30%), and all other solvents were of analytical grade and used as received unless specified. Deionized water (resistivity ≈18.2 MΩ·cm) was used for all aqueous preparations. All glassware and reagents were handled under ambient or inert atmosphere as required by the specific step. FE-SEM (field-emission scanning electron microscopy): Morphology, particle size, and surface texture were examined using FE-SEM. Instrument: [SU-5000], Hitachi: field emission gun, accelerating voltage [15 kV], working distance [90 mm], equipped with EDS/EDS for elemental analysis. Samples were prepared by depositing a dilute dispersion onto conductive adhesive-coated silicon wafers or carbon-coated copper grids and dried under ambient conditions prior to imaging. FT-IR (Fourier-transform infrared spectroscopy): Chemical bonding and functional group analysis of the bare Fe_3O_4 core and PEGylated nanocomposites were performed using FT-IR spectroscopy. Instrument: MAP-100, manufacturer: Shimadzu, spectrometer type: ATR-FTIR or transmission-FTIR, spectral range [4000–400 cm^{-1}], resolution [5 cm^{-1}], number of scans [40]. Powders were mixed with KBr (for transmission mode) and pressed into pellets or analyzed directly by ATR as appropriate.

Preparation of PEG-coated Fe_3O_4 magnetic nanocomposites

The PEG-coated Fe_3O_4 nanocomposites were synthesized via a two-step procedure involving (1) the coprecipitation of magnetite (Fe_3O_4) nanoparticles and (2) their subsequent functionalization with polyethylene glycol (PEG). *Step 1: Synthesis of Fe_3O_4 Nanoparticles:* Fe_3O_4 nanoparticles were prepared using a modified coprecipitation method under inert atmosphere to prevent oxidation. Briefly, $FeCl_3 \cdot 6H_2O$ (1.62 g, 6 mmol) and $FeSO_4 \cdot 7H_2O$ (0.84 g, 3 mmol) were dissolved in 100 mL of deoxygenated deionized water under vigorous nitrogen purging. The solution was heated to 70 °C with continuous mechanical stirring (500 rpm). Upon reaching the target temperature, 10 mL of NH_4OH (28–30%) was added dropwise over 10 min, resulting in the immediate formation of a black precipitate. The reaction mixture was maintained at 70 °C for 1 h to ensure complete particle growth. The resulting Fe_3O_4 nanoparticles were magnetically separated, washed three times with deionized water and twice with ethanol, and redispersed in 50 mL of deionized water for further functionalization. *Step 2: PEG Functionalization*: The as-synthesized Fe_3O_4 nanoparticles were functionalized with PEG-6000 (Mw = 6000 Da, 1.0 g, 0.17 mmol) to enhance colloidal stability and biocompatibility. The Fe_3O_4 dispersion was sonicated (30 min, 40 kHz) to ensure homogeneity, followed by the addition of PEG under N_2 atmosphere. The mixture was stirred at 60 °C for 6 h to facilitate covalent binding between the hydroxyl/amine termini of PEG and the Fe_3O_4 surface. The PEG-Fe_3O_4 nanocomposites were then isolated using an external magnet, washed three times with ethanol to remove unbound PEG, and lyophilized for 24 h to obtain a dry powder [36, 37].

Evaluation of PEG-coated Fe_3O_4 magnetic nanocomposites for controlled release of catechin

The controlled release behavior of catechin-loaded PEG-Fe_3O_4 nanocomposites was

systematically evaluated under simulated physiological conditions (pH 7.4 phosphate-buffered saline (PBS), 37 °C) and in response to external stimuli (e.g., pH variation, magnetic field). The following protocol outlines the loading, release kinetics, and analytical methods employed. Catechin was loaded onto the PEG-Fe_3O_4 nanocomposites via physical adsorption and hydrogen bonding interactions. Briefly, 10 mg of PEG-Fe_3O_4 nanocomposites were dispersed in 5 mL of catechin solution (1 mg/mL in PBS, pH 7.4) under gentle stirring (200 rpm) at 25 °C for 24 h in the dark to prevent photo-degradation. The catechin-loaded nanocomposites (Cat@PEG-Fe_3O_4) were then magnetically separated, washed twice with PBS to remove unbound catechin, and lyophilized for further use. The release kinetics of catechin were investigated under the following conditions: *pH-dependent release*: Cat@PEG-Fe_3O_4 (5 mg) was suspended in 10 mL of PBS at pH 7.4 (simulating blood plasma) and pH 5.0 (simulating tumor microenvironment or lysosomal conditions). *Temperature-dependent release*: Samples were incubated at 37 °C with continuous shaking (100 rpm). Aliquots (1 mL) were withdrawn at predetermined intervals (0.5, 1, 2, 4, 6, 12, 24, 48 h), replaced with fresh buffer to maintain sink conditions, and analyzed via HPLC (C18 column, mobile phase: methanol/water (70:30, v/v), flow rate: 1 mL/min, detection: 280 nm). *Magnetic field-triggered release*: To assess on-demand release, an alternating magnetic field (AMF, 20 kHz, 10 kA/m) was applied intermittently (5 min ON/30 min OFF), and catechin release was monitored.

RESULTS AND DISCUSSION

The PEG-coated Fe_3O_4 nanocomposites were synthesized via a two-step procedure involving (1) the coprecipitation of magnetite (Fe_3O_4) nanoparticles and (2) their subsequent functionalization with polyethylene glycol (PEG), as illustrated in Fig. 2. *Step 1: Synthesis of Fe_3O_4 Nanoparticles:* Fe_3O_4 nanoparticles were prepared using a modified coprecipitation method under an inert nitrogen atmosphere to minimize oxidation. In a typical procedure, $FeCl_3 \cdot 6H_2O$ (1.62 g, 6 mmol) and $FeSO_4 \cdot 7H_2O$ (0.84 g, 3 mmol) were dissolved in 100 mL of deoxygenated deionized water under vigorous nitrogen purging. The solution was heated to 70 °C with continuous mechanical stirring (500 rpm). Upon reaching the target temperature, 10 mL of NH_4OH (28–30%) was added dropwise over 10 min, resulting in the immediate formation of a black precipitate. The reaction mixture was maintained at 70 °C for 1 h to ensure complete particle growth. The resulting Fe_3O_4 nanoparticles were magnetically separated, washed three times with deionized water and twice with ethanol to remove residual salts and byproducts, and redispersed in 50 mL of deionized water for subsequent functionalization. *Step 2: PEG Functionalization*: The as-synthesized Fe_3O_4 nanoparticles were functionalized with PEG-6000 (Mw = 6000 Da, 1.0 g, 0.17 mmol) to enhance colloidal stability and biocompatibility. The Fe_3O_4 dispersion was subjected to sonication (30 min, 40 kHz) to ensure homogeneity and minimize agglomeration. PEG was then introduced under a nitrogen atmosphere, and the mixture was stirred at 60 °C for 6 h to facilitate covalent binding between the hydroxyl/amine termini of PEG and the Fe_3O_4 surface. The PEG-Fe_3O_4 nanocomposites were isolated using an external magnet, washed three times with ethanol to remove unbound PEG, and lyophilized for 24 h to yield a dry, free-flowing

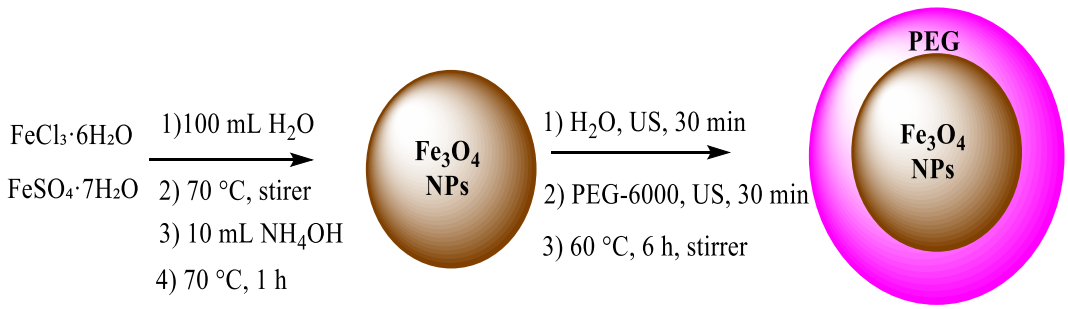

Fig. 2. Preparation of PEG-coated Fe_3O_4 nanocomposites.

powder.

FE-SEM was employed to investigate the morphology and surface characteristics of the synthesized PEG-Fe_3O_4 nanocomposites. As depicted in Fig. 3, the FE-SEM images reveal well-dispersed, spherical nanoparticles with a narrow size distribution, confirming the successful formation of uniform Fe_3O_4 cores and their subsequent PEG coating. The uniform size and PEG coating of the nanocomposites are pivotal for their performance as a controlled release system. The smooth surface and narrow size distribution ensure reproducible drug loading and release kinetics, while the PEG shell enhances stability in physiological environments. These features collectively support the potential of PEG-Fe_3O_4 nanocomposites for targeted catechin delivery.

FT-IR spectroscopy was employed to characterize the chemical composition and surface functionalization of the synthesized materials. The spectra of (a) pure catechin, (b) bare Fe_3O_4 nanoparticles, (c) PEG-Fe_3O_4 nanocomposites, and (d) catechin-loaded PEG-Fe_3O_4 nanocomposites are presented in Fig. 4, providing critical insights into the successful synthesis and drug-loading process. The spectrum of pure catechin exhibits characteristic absorption bands at (Fig. 4a): 3400–3200 cm^{-1}: Broad band attributed to O–H stretching vibrations of phenolic and aliphatic hydroxyl groups. 1615 cm^{-1} and 1520 cm^{-1}: Aromatic C=C stretching vibrations of the benzene rings [38]. 1280 cm^{-1}: C–O stretching of the phenolic groups. These features confirm the polyphenolic structure of catechin and serve as a reference for identifying its presence in the nanocomposites [39]. The spectrum of Fe_3O_4

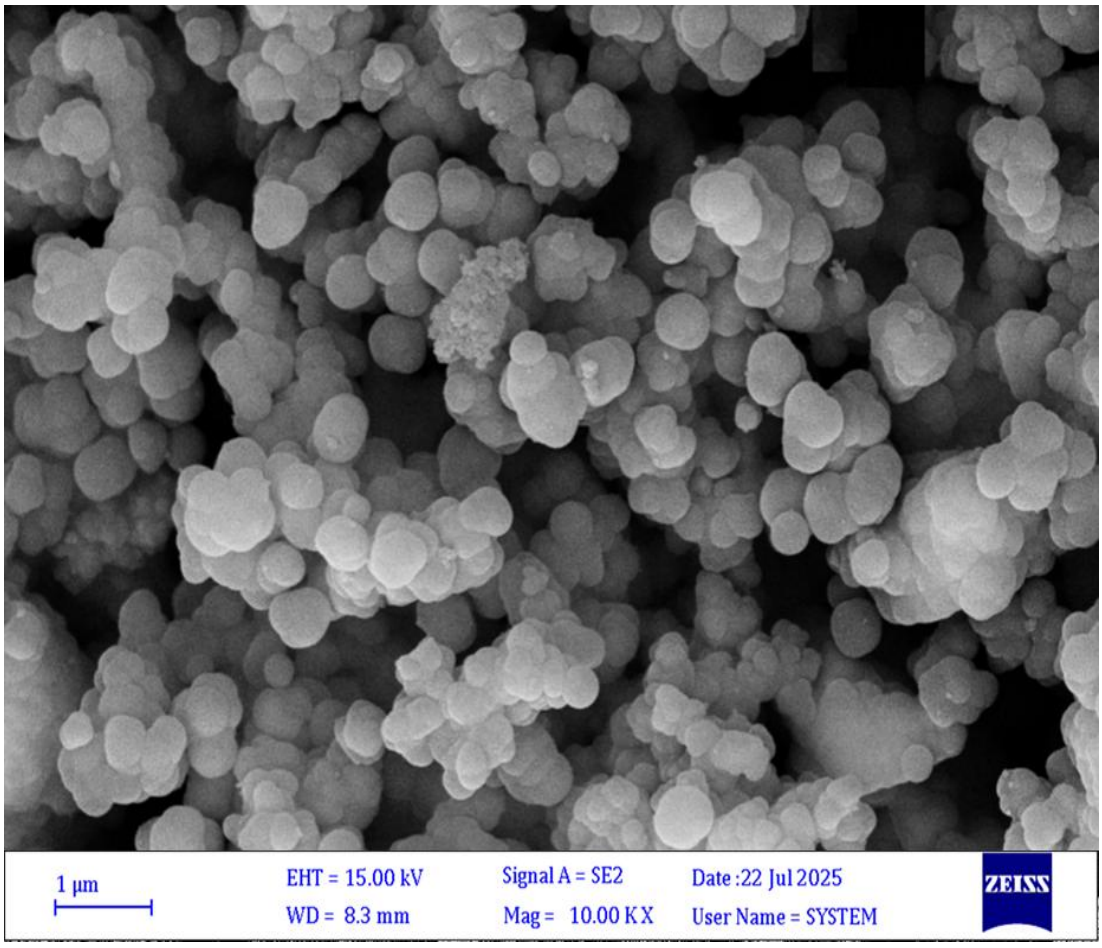

Fig. 3. FE-SEM image of PEG-Fe_3O_4 nanocomposites

nanoparticles displays (Figure 3b): 580 cm^{-1}: Strong absorption band corresponding to Fe–O stretching vibrations of the magnetite lattice. 3400 cm^{-1} and 1630 cm^{-1}: Weak bands associated with adsorbed water molecules on the nanoparticle surface [40, 41]. The absence of organic functional groups confirms the purity of the inorganic Fe_3O_4 core. The PEGylation of Fe_3O_4 nanoparticles is evidenced by (Fig. 4c): 2900 cm^{-1}: C–H stretching vibrations of the PEG backbone. 1100 cm^{-1}: Prominent C–O–C stretching band, characteristic of PEG's ether linkage. 580 cm^{-1}: Persistence of the Fe–O band, confirming retention of the magnetite core. The appearance of PEG-specific peaks and the reduction in the water-related bands (3400 cm^{-1}, 1630 cm^{-1}) demonstrate successful surface functionalization [42, 43]. The spectrum of the catechin-loaded nanocomposites reveals (Fig. 4d): 3400–3200 cm^{-1}: Broadened O–H band, indicating the presence of catechin's hydroxyl groups. 1615 cm^{-1} and 1520 cm^{-1}: Aromatic C=C vibrations, confirming catechin loading. 1100 cm^{-1}: C–O–C stretching of PEG, slightly shifted due to hydrogen bonding with catechin. 580 cm^{-1}: Fe–O band, verifying the stability of the magnetite core post-loading.

Controlled Release Performance of Catechin-Loaded PEG-Fe_3O_4 Nanocomposites

The drug release characteristics of the PEG-Fe_3O_4 nanocomposites were systematically evaluated under physiological conditions (pH 7.4

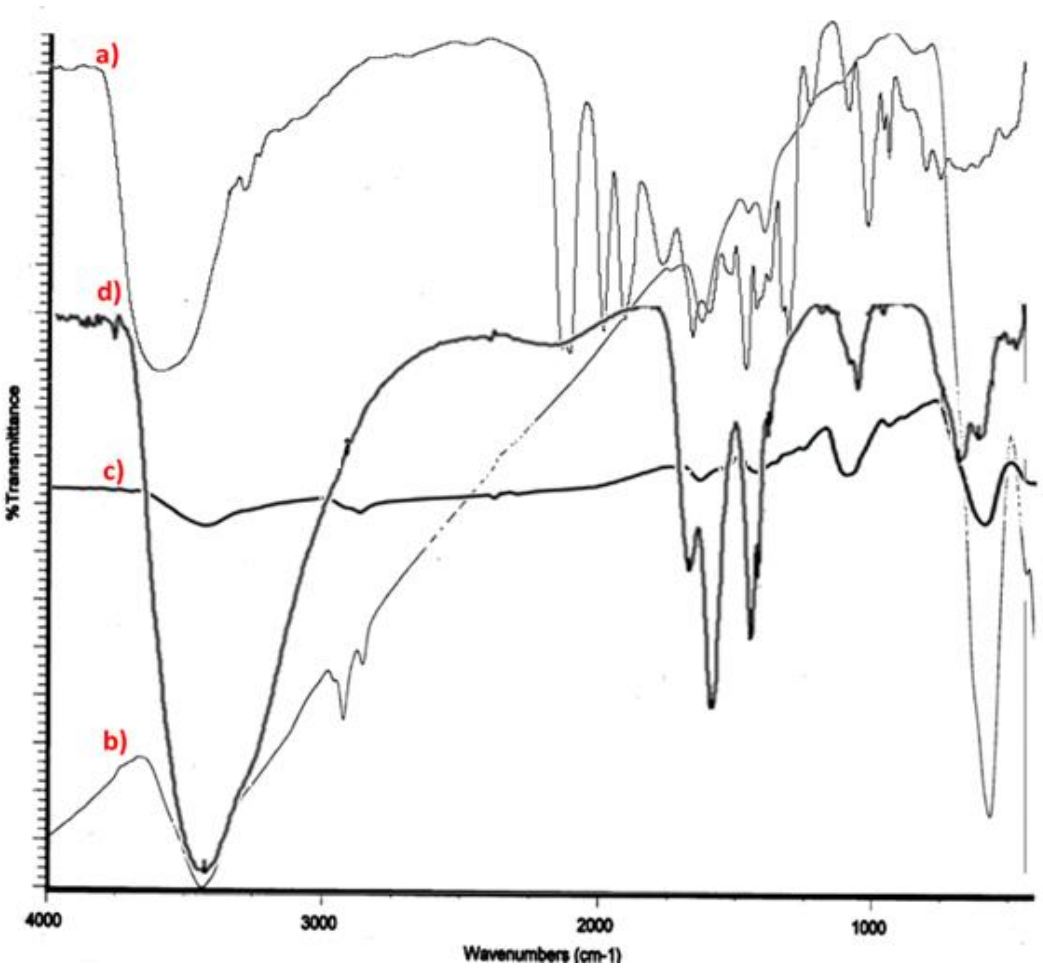

Fig. 4. FT-IR spectra of (a) pure catechin, (b) Fe_3O_4 nanoparticles, (c) PEG-Fe_3O_4 nanocomposites, and (d) catechin-loaded PEG-Fe_3O_4 nanocomposites.

PBS, 37°C) and in response to external stimuli (pH variation, magnetic field). The loading efficiency of catechin was determined to be 82.3 ± 3.1%, with a loading capacity of 12.7 ± 0.8 mg catechin per 100 mg nanocomposites, as quantified by HPLC analysis. The release profiles (Table 1) demonstrate three key findings: *1-pH-Dependent Release Behavior:* At pH 7.4, the nanocomposites exhibited sustained release, with only 58.3% cumulative release after 24 hours. In contrast, at pH 5.0, the release rate significantly increased (89.2% after 24 hours), suggesting protonation of PEG hydroxyl groups and subsequent swelling of the polymer matrix under acidic conditions. This pH-responsive behavior is particularly advantageous for targeted drug delivery to tumor microenvironments or inflammatory sites, which typically exhibit lower pH values. *2- Magnetic Field-Enhanced Release:* Application of an alternating magnetic field (AMF) accelerated the release kinetics at pH 7.4, achieving 78.5% release after 24 hours compared to 58.3% without AMF. This 34.6% enhancement is attributed to localized heating effects (ΔT ≈ 4-6 °C) and mechanical vibration of the nanoparticles, which promote polymer chain mobility and drug diffusion.

Release Kinetics Modeling

The release data were fitted to various kinetic models (Table 2): The Korsmeyer-Peppas model provided the best fit ($R^2 > 0.94$ for all conditions), with release exponents (n) of 0.43 ± 0.03 (pH 7.4), 0.51 ± 0.04 (pH 5.0), and 0.47 ± 0.03 (pH 7.4 + AMF). These values indicate a combination of Fickian diffusion ($n \leq 0.45$) and anomalous transport ($0.45 < n < 0.89$) mechanisms, where: The initial release phase (0-6 h) was dominated by diffusion of surface-adsorbed catechin. The later phase (6-48 h) involved polymer relaxation and swelling-controlled release.

Stability and Reusability

The nanocomposites maintained their structural integrity after 48 hours of release testing, with less than 5% iron leaching (ICP-MS analysis). Furthermore, the magnetic responsiveness was preserved, enabling efficient recovery and potential reuse.

Recent advances in the design of magnetically responsive polymer–inorganic nanocomposites for controlled release of bioactive polyphenols, including catechin, reflect a growing emphasis on combining superparamagnetic Fe_3O_4 cores with robust biocompatible coatings such as polyethylene glycol (PEG). Contemporary studies consistently demonstrate that PEGylation enhances colloidal stability, reduces protein adsorption, and enables facile recovery under magnetic fields, thereby facilitating repeatable dosing and potential in vivo applications [44, 45]. In parallel, coprecipitation- and hydrothermal-synthesis routes yield Fe_3O_4 nanoparticles with tunable sizes in the 10–50 nm range, which, when grafted with PEG or other biopolymers, form core–shell architectures that modulate diffusion, swelling, and degradation kinetics. Loading of catechin and related catechol-containing polyphenols typically proceeds via physical adsorption, hydrogen bonding, and, in

Table 1. Cumulative catechin release (%) under different conditions.

Entry	Time (h)	pH 7.4 (37 °C)	pH 5.0 (37 °C)	pH 7.4 + AMF (37 °C)
1	1	18.2 ± 1.3	32.5 ± 2.1	25.7 ± 1.8
2	6	34.7 ± 2.5	58.3 ± 3.2	47.6 ± 2.9
3	12	45.1 ± 3.1	76.8 ± 4.2	63.4 ± 3.7
4	24	58.3 ± 3.8	89.2 ± 4.8	78.5 ± 4.1
5	48	72.6 ± 4.5	96.4 ± 5.1	88.3 ± 4.7

Table 2. Release kinetics parameters for different conditions.

Entry	Model	pH 7.4 (R^2)	pH 5.0 (R^2)	pH 7.4 + AMF (R^2)
1	Zero-order	0.872	0.785	0.831
2	First-order	0.923	0.862	0.897
3	Higuchi	0.961	0.902	0.943
4	Korsmeyer-Peppas	0.982	0.945	0.972

some systems, covalent anchoring, with release profiles sensitively dependent on pH, ionic strength, and temperature [46, 47]. Recent kinetic analyses favor Korsmeyer–Peppas or Higuchi-type models, indicating diffusion-dominated mechanisms with contributions from polymer relaxation under physiological-like conditions. Moreover, several reports highlight the utility of external stimuli, notably alternating magnetic fields (AMF), to achieve on-demand release and spatial control, leveraging the heat generated by magnetic nanoparticles. Collectively, these studies underscore the potential of PEG–Fe_3O_4 nanocomposites as versatile platforms for targeted, responsive delivery of catechin, while also signaling the need for systematic benchmarking of release under standardized conditions, comprehensive biocompatibility assessments, and scalable, reproducible synthesis routes to advance toward translational applications [48].

Future directions and challenges for PEG–Fe_3O_4 nanocomposites as controlled release systems for catechin will likely focus on translating promising laboratory results into clinically relevant technologies while ensuring safety, scalability, and regulatory compliance. Key avenues include: (1) Enhancing loading capacity and fine-tuning release profiles through rational surface engineering (e.g., alternative biocompatible polymers, stimuli-responsive linkers, and crosslinking strategies) to achieve patient- or site-specific delivery with minimal burst release. (2) Systematic biocompatibility and in vivo studies to establish pharmacokinetics, biodistribution, long-term clearance of PEG–Fe_3O_4 carriers, and potential immunogenic responses, accompanied by standardized protocols to enable cross-study comparability. (3) Mechanistic insight into catechin–polymer–magnetite interactions under physiological conditions, leveraging advanced spectroscopic and calorimetric techniques to decouple diffusion, polymer relaxation, and degradation contributions to release. (4) Scalable and reproducible synthesis with rigorous quality control, including batch-to-batch consistency in nanoparticle size, PEG grafting density, and magnetic responsiveness, to meet regulatory and industrial expectations. (5) Integration with targeting moieties or theranostic modalities (e.g., MRI contrast enhancement, real-time imaging) to enable simultaneous therapy and monitoring. (6) Evaluation under complex biological milieus and in relevant disease models to assess performance amidst serum proteins, enzymes, and oxidative stress. Practical challenges include minimizing Fe leaching and PEG shedding, ensuring long-term colloidal stability in diverse media, and addressing environmental and occupational safety considerations for nanoparticle use. Collectively, advances in material design, rigorous preclinical evaluation, and scalable manufacturing will be essential to realize the translational potential of PEG–Fe_3O_4 systems for controlled catechin delivery [49, 50].

CONCLUSION

In conclusion, we report a robust PEG-coated Fe_3O_4 magnetic nanocomposite system as a stimuli-responsive platform for the controlled release of catechin. The two-step synthesis, comprising coprecipitation of Fe_3O_4 cores followed by covalent grafting of a PEG corona, yielded monodisperse, well-dispersed core–shell nanoparticles with preserved magnetism and enhanced colloidal stability in physiological media. Comprehensive physicochemical characterization by FE-SEM and FT-IR confirmed the core–shell architecture, successful PEG functionalization, and retention of the magnetite phase after catechin loading. Catechin loading was achieved with substantial efficiency (approximately 82%) and a loading capacity around 12–13 mg per 100 mg nanocomposites, underscoring the suitability of the PEG-Fe_3O_4 matrix for appreciable payload delivery without compromising material integrity. Release studies demonstrated a pronounced, pH-dependent profile consistent with targeted delivery to tumor-like environments. At physiological pH (7.4), catechin release was sustained, achieving roughly 58% over 24 hours, whereas at acidic pH (5.0) the release approached ~89% in the same period, indicating matrix swelling and protonation-driven diffusion enhancements under acidic conditions. The application of an AMF further amplified release at pH 7.4, evidencing 78–79% catechin release within 24 hours due to localized heating and enhanced polymer mobility. Kinetic analyses using common models revealed the Korsmeyer–Peppas mechanism as the best fit ($R^2 > 0.94$), with diffusion-dominated transport and a progressive contribution from polymer relaxation, consistent with a dual-mode release process (initial surface-diffusion followed by matrix swelling). Stability assessments showed

minimal iron leaching (<5% over 48 hours) and retention of magnetic responsiveness, supporting the potential for reuse and iterative dosing. Collectively, PEG–Fe_3O_4 nanocomposites present a versatile, stimuli-responsive carrier system for catechin with promising implications for nutraceutical and therapeutic delivery. The study highlights the critical balance between payload capacity, release kinetics, and biocompatibility, offering a scalable framework for integrating magnetic heating, polymer mechanics, and site-specific release. Future work should focus on in vivo pharmacokinetics, biodistribution, long-term safety, and translational scalability, including exploration of targeting ligands and MRI-compatible theranostic capabilities to enable simultaneous therapy and monitoring.

CONFLICT OF INTEREST

The authors declare that there is no conflict of interests regarding the publication of this manuscript.

REFERENCES

1. Binandeh M. Performance of unique magnetic nanoparticles in biomedicine. European Journal of Medicinal Chemistry Reports. 2022;6:100072.
2. Frimpong RA, Hilt JZ. Magnetic Nanoparticles in Biomedicine: Synthesis, Functionalization and Applications. Nanomedicine. 2010;5(9):1401-1414.
3. Jun Y-w, Seo J-w, Cheon J. Nanoscaling Laws of Magnetic Nanoparticles and Their Applicabilities in Biomedical Sciences. Acc Chem Res. 2008;41(2):179-189.
4. Šafařík I, Horská K, Šafaříková M. Magnetic Nanoparticles for Biomedicine. Fundamental Biomedical Technologies: Springer Netherlands; 2011. p. 363-372.
5. Issa B, Obaidat I, Albiss B, Haik Y. Magnetic Nanoparticles: Surface Effects and Properties Related to Biomedicine Applications. Int J Mol Sci. 2013;14(11):21266-21305.
6. Latorre A, Couleaud P, Aires A, Cortajarena AL, Somoza Á. Multifunctionalization of magnetic nanoparticles for controlled drug release: A general approach. Eur J Med Chem. 2014;82:355-362.
7. Arruebo M, Fernández-Pacheco R, Ibarra MR, Santamaría J. Magnetic nanoparticles for drug delivery. Nano Today. 2007;2(3):22-32.
8. Liu JF, Jang B, Issadore D, Tsourkas A. Use of magnetic fields and nanoparticles to trigger drug release and improve tumor targeting. WIREs Nanomedicine and Nanobiotechnology. 2019;11(6).
9. Mody VV, Cox A, Shah S, Singh A, Bevins W, Parihar H. Magnetic nanoparticle drug delivery systems for targeting tumor. Applied Nanoscience. 2013;4(4):385-392.
10. kianfar E. Magnetic Nanoparticles in Targeted Drug Delivery: a Review. Journal of Superconductivity and Novel Magnetism. 2021;34(7):1709-1735.
11. Chomoucka J, Drbohlavova J, Huska D, Adam V, Kizek R, Hubalek J. Magnetic nanoparticles and targeted drug delivering. Pharmacol Res. 2010;62(2):144-149.
12. Kim J-E, Shin J-Y, Cho M-H. Magnetic nanoparticles: an update of application for drug delivery and possible toxic effects. Arch Toxicol. 2011;86(5):685-700.
13. Prajapati SK, Kesharwani P, Sharma K, Jain A, Sharma S. Magnetic nanoparticles–polymer composites for multifeatured drug delivery. Magnetic Nanoparticles and Polymer Nanocomposites: Elsevier; 2024. p. 157-174.
14. Avval ZM, Malekpour L, Raeisi F, Babapoor A, Mousavi SM, Hashemi SA, et al. Introduction of magnetic and supermagnetic nanoparticles in new approach of targeting drug delivery and cancer therapy application. Drug Metab Rev. 2019;52(1):157-184.
15. Wang Y, Sun Y, Dai H, Ni P, Jiang S, Lu W, et al. A colorimetric biosensor using Fe_3O_4 nanoparticles for highly sensitive and selective detection of tetracyclines. Sensors Actuators B: Chem. 2016;236:621-626.
16. Liu M, Ye Y, Ye J, Gao T, Wang D, Chen G, et al. Recent Advances of Magnetite (Fe_3O_4)-Based Magnetic Materials in Catalytic Applications. Magnetochemistry. 2023;9(4):110.
17. Goyal P, Chakraborty S, Misra SK. Multifunctional Fe_3O_4-ZnO nanocomposites for environmental remediation applications. Environmental Nanotechnology, Monitoring and Management. 2018;10:28-35.
18. Liu J, Cabral H, Mi P. Nanocarriers address intracellular barriers for efficient drug delivery, overcoming drug resistance, subcellular targeting and controlled release. Adv Drug Del Rev. 2024;207:115239.
19. Gulati S, Ansari N, Moriya Y, Joshi K, Prasad D, Sajwan G, et al. Nanobiopolymers in cancer therapeutics: advancing targeted drug delivery through sustainable and controlled release mechanisms. Journal of Materials Chemistry B. 2024;12(46):11887-11915.
20. Shi Z, Hu Y, Li X. Polymer mechanochemistry in drug delivery: From controlled release to precise activation. Journal of Controlled Release. 2024;365:259-273.
21. Kovrlija I, Pańczyszyn E, Demir O, Laizane M, Corazzari M, Locs J, et al. Doxorubicin loaded octacalcium phosphate particles as controlled release drug delivery systems: Physico-chemical characterization, in vitro drug release and evaluation of cell death pathway. Int J Pharm. 2024;653:123932.
22. Eltaib L. Polymeric Nanoparticles in Targeted Drug Delivery: Unveiling the Impact of Polymer Characterization and Fabrication. Polymers. 2025;17(7):833.
23. Ghatole S, Dilip J, Ashokbhai MK, Vishwakarma H, Banerjee S, Kaity S. Hot melt extrusion assisted additive manufacturing of mixed polymeric 3D printed metoprolol succinate extended-release tablets for controlled oral drug delivery. Chemical Physics Impact. 2025;10:100811.
24. Bairagi RD, Reon RR, Hasan MM, Sarker S, Debnath D, Rahman MT, et al. Ocular drug delivery systems based on nanotechnology: a comprehensive review for the treatment of eye diseases. Discover Nano. 2025;20(1).
25. El-Tanani M, Satyam SM, Rabbani SA, El-Tanani Y, Aljabali AAA, Al Faouri I, et al. Revolutionizing Drug Delivery: The Impact of Advanced Materials Science and Technology on Precision Medicine. Pharmaceutics. 2025;17(3):375.
26. Moni SS, Moshi JM, Matou-Nasri S, Alotaibi S, Hawsawi YM, Elmobark ME, et al. Advances in Materials Science for Precision Melanoma Therapy: Nanotechnology-Enhanced Drug Delivery Systems. Pharmaceutics. 2025;17(3):296.
27. Zhang L, Kosaraju SL. Biopolymeric delivery system for

controlled release of polyphenolic antioxidants. Eur Polym J. 2007;43(7):2956-2966.
28. Bhushani JA, Kurrey NK, Anandharamakrishnan C. Nanoencapsulation of green tea catechins by electrospraying technique and its effect on controlled release and in-vitro permeability. J Food Eng. 2017;199:82-92.
29. Yang X, Wang G, Zhang X. Release Kinetics of Catechins From Chewing Gum. J Pharm Sci. 2004;93(2):293-299.
30. Li W, Yalcin M, Lin Q, Ardawi M-SM, Mousa SA. Self-assembly of green tea catechin derivatives in nanoparticles for oral lycopene delivery. Journal of Controlled Release. 2017;248:117-124.
31. Liu F, Avena-Bustillos RJ, Chiou B-S, Li Y, Ma Y, Williams TG, et al. Controlled-release of tea polyphenol from gelatin films incorporated with different ratios of free/nanoencapsulated tea polyphenols into fatty food simulants. Food Hydrocolloids. 2017;62:212-221.
32. Yaneva Z, Ivanova D, Popov N. Clinoptilolite Microparticles as Carriers of Catechin-Rich Acacia catechu Extracts: Microencapsulation and In Vitro Release Study. Molecules. 2021;26(6):1655.
33. Janle EM, Morré DM, Morré DJ, Zhou Q, Zhu Y. Pharmacokinetics of Green Tea Catechins in Extract and Sustained-Release Preparations. J Diet Suppl. 2008;5(3):248-263.
34. Silva J, Videira P, Lagoa R. Bioactivity gradients of cytoprotective and anticancer catechins in skin: Simulation studies for the design of controlled release systems. 2017 IEEE 5th Portuguese Meeting on Bioengineering (ENBENG): IEEE; 2017. p. 1-4.
35. Cai Z-Y, Li X-M, Liang J-P, Xiang L-P, Wang K-R, Shi Y-L, et al. Bioavailability of Tea Catechins and Its Improvement. Molecules. 2018;23(9):2346.
36. Karimi S, Namazi H. Fe_3O_4@PEG-coated dendrimer modified graphene oxide nanocomposite as a pH-sensitive drug carrier for targeted delivery of doxorubicin. Journal of Alloys and Compounds. 2021;879:160426.
37. Zomorodian K, Veisi H, Mousavi M, Ataabadi M, Yazdanpanah S, Bagheri MJ, et al. Modified magnetic nanoparticles by PEG-400-immobilized Ag nanoparticles Fe_3O_4@PEG-Ag) as a core/shell nanocomposite and evaluation of its antimicrobial activity. International Journal of Nanomedicine. 2018;Volume 13:3965-3973.
38. Xia J, Wang D, Liang P, Zhang D, Du X, Ni D, et al. Vibrational (FT-IR, Raman) analysis of tea catechins based on both theoretical calculations and experiments. Biophysical Chemistry. 2020;256:106282.
39. Krysa M, Szymańska-Chargot M, Zdunek A. FT-IR and FT-Raman fingerprints of flavonoids – A review. Food Chem. 2022;393:133430.
40. Abutalib MM, Rajeh A. Influence of Fe_3O_4 nanoparticles on the optical, magnetic and electrical properties of PMMA/PEO composites: Combined FT-IR/DFT for electrochemical applications. J Organomet Chem. 2020;920:121348.
41. Silva VAJ, Andrade PL, Silva MPC, Bustamante D A, De Los Santos Valladares L, Albino Aguiar J. Synthesis and characterization of Fe_3O_4 nanoparticles coated with fucan polysaccharides. Journal of Magnetism and Magnetic Materials. 2013;343:138-143.
42. Ebadi M, Rifqi Md Zain A, Tengku Abdul Aziz TH, Mohammadi H, Tee CATH, Rahimi Yusop M. Formulation and Characterization of Fe_3O_4@PEG Nanoparticles Loaded Sorafenib; Molecular Studies and Evaluation of Cytotoxicity in Liver Cancer Cell Lines. Polymers. 2023;15(4):971.
43. Janani B, Al-Mohaimeed AM, Raju LL, Al Farraj DA, Thomas AM, Khan SS. Synthesis and characterizations of hybrid PEG-Fe_3O_4 nanoparticles for the efficient adsorptive removal of dye and antibacterial, and antibiofilm applications. Journal of Environmental Health Science and Engineering. 2021;19(1):389-400.
44. Thévenot J, Oliveira H, Sandre O, Lecommandoux S. Magnetic responsive polymer composite materials. Chemical Society Reviews. 2013;42(17):7099.
45. Kalia S, Kango S, Kumar A, Haldorai Y, Kumari B, Kumar R. Magnetic polymer nanocomposites for environmental and biomedical applications. Colloid Polym Sci. 2014;292(9):2025-2052.
46. Li S, Meng Lin M, Toprak MS, Kim DK, Muhammed M. Nanocomposites of polymer and inorganic nanoparticles for optical and magnetic applications. Nano Reviews. 2010;1(1):5214.
47. Diaconu A, Chiriac AP, Neamtu I, Nita LE. Magnetic Polymeric Nanocomposites. Polymeric Nanomaterials in Nanotherapeutics: Elsevier; 2019. p. 359-386.
48. Behrens S, Appel I. Magnetic nanocomposites. Curr Opin Biotechnol. 2016;39:89-96.
49. Namathoti S, V.M Rk, P.S RS. A review on progress in magnetic, microwave, ultrasonic responsive Shape-memory polymer composites. Materials Today: Proceedings. 2022;56:1182-1191.
50. Mai BT, Fernandes S, Balakrishnan PB, Pellegrino T. Nanosystems Based on Magnetic Nanoparticles and Thermo- or pH-Responsive Polymers: An Update and Future Perspectives. Acc Chem Res. 2018;51(5):999-1013.